Structure of the cro repressor from bacteriophage λ and its interaction with DNA

W. F. Anderson*†, D. H. Ohlendorf*, Y. Takeda‡ & B. W. Matthews*

* Institute of Molecular Biology and Department of Physics, University of Oregon, Eugene, Oregon 97403, USA
† MRC Group on Protein Structure and Function, Department of Biochemistry, University of Alberta, Edmonton, Alberta, Canada T6G 2H7
‡ Chemistry Department, University of Maryland, Baltimore County, Catonsville, Maryland 21228, USA

The three-dimensional structure of the 66-amino acid cro repressor protein of bacteriophage λ suggests how it binds to its operator DNA. We propose that a dimer of cro protein is bound to the B-form of DNA with the 2-fold axis of the dimer coincident with the 2-fold axis of DNA. A pair of 2-fold-related α-helices of the repressor, lying within successive major grooves of the DNA, seem to be a major determinant in recognition and binding. In addition, the C-terminal residues of the protein, some of which are disordered in the absence of DNA, appear to contribute to the binding.

INTERACTIONS between proteins and nucleic acids are of central importance in molecular biology. Some proteins bind single-stranded polynucleotides while others recognize double-stranded ones. None of these interactions is well understood in molecular terms. In particular, the way in which proteins recognize specific base sequences within double-stranded DNA has remained enigmatic.

The cro protein from bacteriophage λ (hereafter called 'cro') is a repressor molecule which recognizes and binds tightly certain sequence-specific operator regions within the DNA of the bacteriophage. Cro is the smallest repressor protein that has been characterized, and is of interest both because of its role in the delicately balanced regulatory system of bacteriophage λ, and as a general model for protein–DNA interaction.

We describe here the three-dimensional structure of the cro repressor and its apparent mode of interaction with operator DNA. The postulated interaction between repressor and operator is consistent with a variety of chemical and genetic evidence, and may provide a general model for the interaction of proteins with helical DNA.

The bacteriophage λ genome encodes two repressor proteins that play essential, contrasting parts in regulating the development of the phage. The product of the *c*I gene, the cI or λ repressor ('cI'), is required for the maintenance of the lysogenic state, whereas the product of the *cro* gene is necessary during the lytic cycle of phage development (for reviews see refs 1–4, 33, 34). Both the cro and the cI repressors compete for and bind two operator regions within the phage genome. These operator regions each consist of three binding sites for the repressor molecules, and the respective repressors have different relative affinities for each of the sites within the operator regions[5,6]. The use of these binding sites by cro and cI provides for a switch between the lysogenic and lytic pathway. The cro/cI interaction is the clearest example of such a developmental switch[33] and the structural results presented here begin an understanding of this switch at the molecular level.

The cro protein is well characterized[7,8]. It is a small basic protein 66-amino acid residues long, with a monomer molecular weight of 7,351. Both the amino acid sequence of the protein[9] and the nucleotide sequence of the *cro* gene have been determined[10].

Structure determination

The structure was determined by the method of isomorphous replacement[11–13]. Protein purification and crystallization from 1.1 to 1.3 M phosphate were as described previously[8,14]. The space group is R32 and the cell dimensions in the hexagonal system $a = b = 91.9$ Å, $c = 268.9$ Å.

Potential heavy-atom derivatives were initially screened by precession photography, and, later, by using a diffractometer to collect 5-Å-resolution data sets. The first heavy-atom derivative to be interpreted was obtained using $PtCl_4^{2-}$ and was initially solved by a 'brute force' approach in which all possible individual sites, and then combinations of sites, were explored (ref. 15 and unpublished results of B.W.M.). Using the phases obtained from this platinum derivative, other potential derivatives were then evaluated in the normal way[12,13]. In the end, five derivatives were selected for high-resolution data collection (Table 1). All the derivatives have multiple binding sites, as expected with multiple copies of the protein present in the crystallographic asymmetric unit (see below). Higher-resolution data were collected by oscillation photography[16] which permitted collection of data sets to a nominal resolution of 2.8 Å or better from a single crystal. The crystals often grow as long triangular prisms[14], in which case they can be translated between series of exposures. Some data collection statistics are included in Table 1.

Two preliminary electron density maps to 5 Å resolution were calculated, one using the data collected by diffractometry, and the other using a subset of the higher-resolution oscillation data. The two maps were quite similar, and, as discussed below, were important in working out the arrangement of the cro monomers within the crystallographic asymmetric unit.

Molecular symmetry

The initial analysis of the cro protein crystals showed them to contain multiple copies of the protein in the asymmetric unit. On the basis of the density measurement of two cross-linked crystals, there seemed to be six monomers, that is, three dimers, per asymmetric unit[14]. However, examination of the 5 Å-resolution electron density map revealed that there were four monomers per asymmetric unit, not six. The error in the previous estimate could be due either to the presence of the cross-linking agent or to errors in density due to the limited amount of material available.

We attempted to determine the relation between the monomers in two ways—by inspection of the 5-Å-resolution electron density maps, and by consideration of the relation between the sites of heavy-atom binding. Initial inspection of the 5-Å-resolution map revealed an obvious 2-fold symmetry

Table 1 Heavy-atom derivatives

Derivative	No. of sites	R_{Merge} (%)	R_{Der} (%)	Reflections above 3σ	R_{wc} (%)	$\langle f_H \rangle$	E
Native	—	9.5	—	9184			
$PtCl_4^{2-}$	6	9.6	14.5	5068	30.5	64.3	54.5
Hg^{2+}	16	8.9	12.9	3616	44.9	113.4	72.4
Au^{2+}	16	8.7	14.0	7273	47.1	59.5	46.8
EMTS	12	0.3	11.0	7856	48.7	39.0	32.2
Mersalyl	13	10.2	14.0	5985	46.1	62.5	51.5

Overall figure of merit[18] to 2.8 Å resolution, 0.45. $R_{Merge} = 100 \sum (I_i - \langle I \rangle) / \sum \langle I \rangle$, $R_{Der} = 200 \sum |I_{PH} - I_P| / \sum (I_{PH} + I_P)$, $R_{wc} = 100 \sum \omega | |F_{PH}| - F_P| - f_H| / \sum \omega |F_{PH} - F_P|$. $\langle f_H \rangle$ is the mean heavy-atom scattering, E the average lack of closure for centric reflections[18]. EMTS, ethyl mercury thiosalicic acid. Hg^{2+} data set collected by precession photography.

0028-0836/81/180754—05$01.00

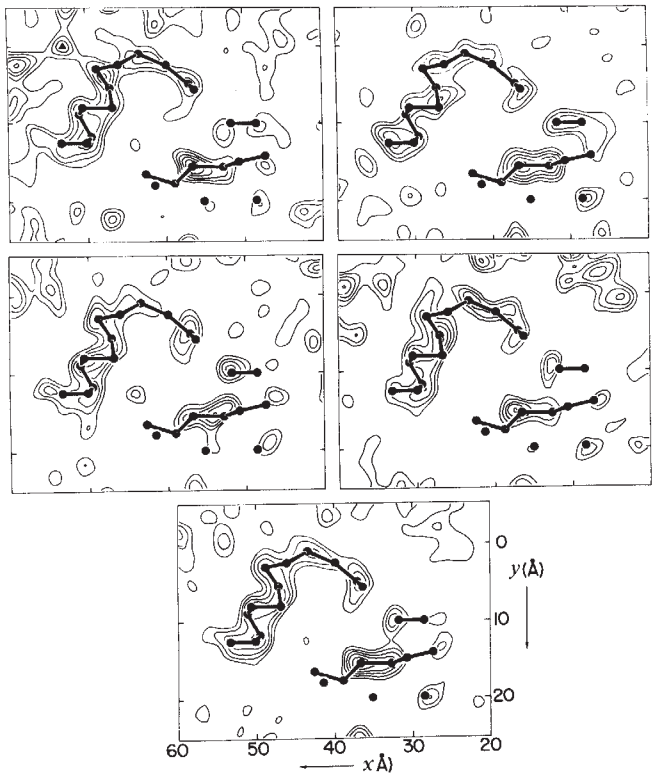

Fig. 1 Corresponding electron density sections through each of the four cro molecules in the crystallographic asymmetric unit, transformed into a common coordinate frame. Clockwise from top left the density is for molecules O, A, B and C, with the averaged density below. α-carbon atoms within ±2.5 Å of the section are indicated by the solid circles.

axis lying approximately in the plane $z = 1/12$. This 2-fold axis also related, in pairs, most of the major heavy-atom sites. Further analysis of the 5-Å map, facilitated by the use of an MMS-X computer graphics system[17], suggested that there were two additional 2-fold axes inclined to the first. The positions of these local symmetry elements were confirmed by calculating correlation coefficients between the electron density of the individual monomers, rotated and translated to superimpose one monomer on another (Table 2). The four monomers are related in pairs by mutually perpendicular intersecting (or nearly intersecting) 2-fold axes. In other words, the four monomers are arranged in the crystal with local 222-point symmetry. The symmetry of the molecules in the crystal does not itself imply anything about the state of aggregation in solution. In principle, the protein could exist as individual monomers, as dimers with 2-fold symmetry, or as tetramers. However, the specific interactions which we observed between the four monomers (see below) suggests that cro may exist in solution as a tetramer. The extent to which the molecular arrangement may depart from exact 222 symmetry, and the potential biological relevance of such deviations from exact symmetry, remain to be determined.

Most, but not all, of the heavy-atom sites are related to each other by the 222 local symmetry elements. For each 2-fold axis, related pairs of sites can be superimposed within ~1.9 Å (Table 2). Although the 2-fold symmetry was used as an additional check in the interpretation of the heavy-atom derivatives, it was not imposed on the heavy-atom coordinates.

The electron density map

An electron density map was calculated to a nominal resolution of 2.8 Å using the five heavy-atom derivatives described in Table 1 (ref. 18). Although the phase angles are well determined to about 3.5 Å resolution, their accuracy at higher angles is limited by the scattering intensity of the derivative crystals, which becomes very weak at higher resolution, and also, in part, by non-isomorphism.

To improve the accuracy of the electron density map and facilitate its initial interpretation, the density of the four monomers in the asymmetric unit was averaged (Table 2, Fig. 1). If the assumed transformations are correct and all four monomers are, in fact, identical, the averaging process should improve the accuracy of the electron density map. In practice, the averaging process clearly improved the overall 'cleanliness' of the map, but also resulted in a loss of detail and reduction in the effective resolution (Fig. 1). Presumably, application of more sophisticated averaging techniques[19] and refinement of the individual monomers will lead to a more precise description of the structure.

The averaged electron density map was displayed both as a 'mini-map' and on a scale of 2 cm = 1 Å in an optical comparator[20,21]. Several helices and a region of β-sheet were immediately apparent, and the course of the polypeptide backbone could be readily followed from one end to the other. The direction of the polypeptide chain was initially deduced from the observation that the major platinum binding site was at a position 12 residues from one terminus, obviously corresponding to Met 12. From this point the known amino acid sequence of the protein[9,10] could be compared with the electron density map. Although the interpretation of the electron density map is fully consistent with the sequence, note that the limited resolution of the current map, together with the averaging process described above, results in poorly defined density for the respective side chains. The backbone density is strong and unambiguous from the amino terminus to residue Lys 62, but at this point the density becomes very weak, indicating that the four carboxy-terminal residues are disordered in the crystals. This appears to be the case for each of the four cro monomers.

Conformation of the cro repressor

The conformation of a cro monomer is illustrated in Fig. 2. The structure is very simple, consisting of three strands of antiparallel β-sheet (residues 2–6, 39–45 and 48–55), and three α-helices (residues 7–14, 15–23 and 27–36). As described below, the C-terminal residues form an extended 'arm' (Fig. 2) which interacts with another monomer and seems to participate in DNA binding.

The detailed arrangement of the four repressor monomers in the crystals is shown in Fig. 7. The respective local 2-fold symmetry axes relating the monomers are designated P, Q and R, and the monomers themselves O ('original'), A, B and C (Table 2). It has been assumed for some time that the cro

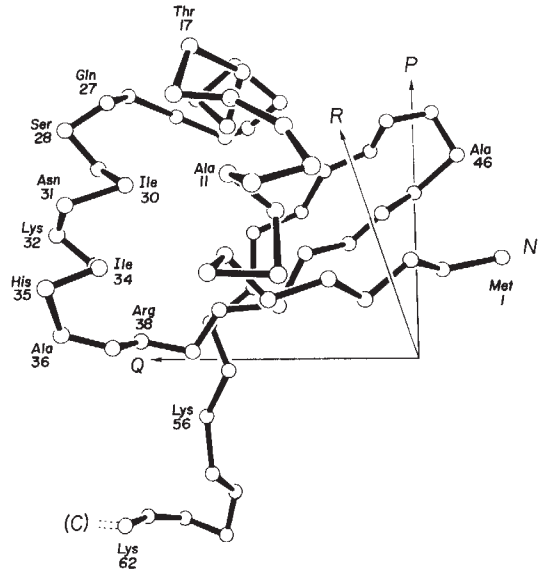

Fig. 2 Backbone of monomer O of the cro repressor protein. As discussed in the text, the four C-terminal residues 63–66 are disordered. The local orthogonal 2-fold symmetry axes P, Q and R relate the molecule shown to monomers A, B and C, respectively.

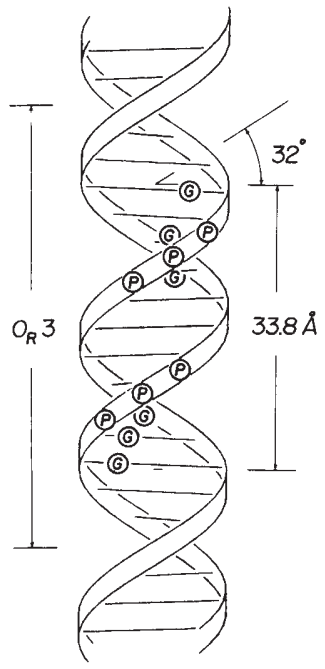

Fig. 3 DNA operator O_R3, drawn in the B form (after Ptashne *et al.*[4]). Ethylation of the phosphates, labelled P, hinders cro repressor binding; binding of cro protects the N^7 positions of guanines, labelled G, from methylation by dimethyl sulphate. The figure is based on experiments of Johnson, Ptashne and collaborators.[4,5,35].

repressor exists as a dimer in physiological conditions[8]. Therefore, we expected the four cro monomers in the crystal to consist of two dimers. However, inspection of the molecular packing does not obviously support this assumption. The monomers O and B (and, similarly A and C) are related by the Q axis, and have extensive interactions between their C-terminal arms, each of which lies against, and is, in part, hydrogen bonded to, its 2-fold-related partner. It seems likely that this interaction persists in solution. However, there are also specific interactions about the R symmetry axis, where the polypeptide backbone of one monomer hydrogen bonds to the 2-fold-related backbone of the other monomer so as to expand the three-strand β-sheet of the monomer into a six-strand antiparallel sheet in the dimer. In addition, the amino terminus of monomer O is linked by an ionic interaction to Glu 53 of monomer A, with similar interactions for the other amino termini. The four amino-terminal methionines are grouped together and participate in a distinct hydrophobic region at the centre of the cro tetramer. Thus, although the packing arrangement seen in the crystal does not prove that cro exists as a tetramer in solution, it does suggest this. Whether cro exists as a dimer or tetramer has no bearing on the proposed model for DNA binding.

Interaction of cro with DNA

Both cI and cro repressors compete for three sites within the left and the right operators of bacteriophage λ. In the right operator there are three binding sites (O_R1, O_R2 and O_R3) each consisting of 17-base pair regions separated by spacers of 6 or 7 base pairs[22]. The sequences of the three 17-base pair regions are similar to each other, but not identical, and, in addition, the sequence within each region is approximately symmetric. Mutations within the 17-base pair regions reduce the binding affinity of both cro and cI, whereas mutations in the spacer regions have no effect on binding (refs 4, 6, 23, 24 and refs therein). Chemical probe experiments[4,5,35] indicate that both cro and cI repressors bind primarily along one face of the DNA double helix and protect many of the same groups. The results of such experiments for cro binding to O_R3 are illustrated in Fig. 3. Methylation by dimethyl sulphate of the N^7 of six guanines in the major groove is prevented by the presence of cro, but methylation of N^3 of adenine, exposed in the minor groove of the DNA, is not prevented. Furthermore, ethylation of any of the six phosphates shown in Fig. 3 interferes with cro binding[4]. The pattern for cI is very similar, but is slightly more extended, and includes four additional phosphates. Such experiments suggest that both cro and cI contact the DNA in the major, but not the minor, groove[4,5]. Furthermore, it seems likely that both repressors bind to the DNA with two symmetry-related subunits of the protein in contact with the two symmetry-related halves of the operator, and the 2-fold axis of the protein coincident with the 2-fold axis of the DNA. In this way the complex of bound repressor and operator would have a common 2-fold symmetry axis. There would, of course, be slight deviations from exact 2-fold symmetry because of the inexact symmetry of the DNA base sequence, and also, possibly, due to the protein.

To determine possible modes of binding of cro to DNA, we looked for a feature of the cro monomer which, together with its 2-fold related mate, would form a structure complementary to that of the operator DNA, and which, when aligned on the DNA, would be consistent with the protection experiments summarized in Fig. 3. An obvious candidate is the helix from residues Gln 27 to Ala 36. This helix lies along the surface of the protein, with isoleucines 30 and 34 contributing to the hydrophobic interior of the monomer, but with the helix otherwise protruding from the surface of the protein (Fig. 2). The corresponding helix in monomer B, related by rotation about axis Q (Fig. 4) is parallel, and the respective helices have a centre-to-centre distance of 34 Å, the same as the separation between successive major grooves of B-form DNA (Fig. 3). Furthermore, the angle made between the axes of the two α-helices and the line connecting their midpoints is equal to the angle between the major groove of the DNA and its long axis (Figs 3, 4). The sense of the respective angles is such that the two helices can be accommodated, in a very natural way, within successive major grooves of DNA in its normal Watson–Crick B conformation[25,26].

This hypothetical arrangement was checked by fitting a model of the cro molecule to that of DNA. We required that the 2-fold axis relating the cro monomers had to coincide with the 2-fold axis through the centre of the DNA operator. Thus, the fitting of cro to the DNA is very restrictive, allowing only two degrees of freedom—one a rotation of cro relative to the DNA, about the common symmetry axis; the second a translation of cro along the symmetry axis, which varies the distance between cro and the long axis of the DNA. The results of this first, albeit crude, fitting process are shown in Figs 5, 6 and 7.

The complementarity between protein and DNA is striking. In addition to the overall correspondence between the respective backbones of the DNA and protein, residues Ser 28, Ala 29, Asn 31, Lys 32, Ala 33 and His 35 of the above-mentioned α-helix are in a position to interact either with the exposed hydrogen bonding groups of the major groove, conferring specificity, or with the negatively charged phosphates, promoting generalized binding. Nearby residues, including Arg 38 and Lys 39, are also suitably located to contribute to binding and recognition. Close to the 2-fold symmetry axis, the sequences Glu 54–Val 55–Lys 56 of the two monomers form a pair of antiparallel β-sheet strands parallel to the minor groove which possibly interact with the DNA in the manner proposed

Table 2 Relations between the four cro monomers

Symmetry axis	Pairs of heavy-atom sites	r.m.s. error in heavy-atom sites	Monomers related	Electron density correlation
P	26	1.80	O,A	0.58
Q	26	1.97	O,B	0.54
R	25	1.94	O,C	0.55

$C_{ij} = \sum \rho_i \rho_j / (\sum \rho_i^2 . \sum \rho_j^2)^{1/2}$ where the summations are over all values, ρ_i, of the 2.8 Å-resolution electron density map within 15 Å of the centre of the respective monomers.

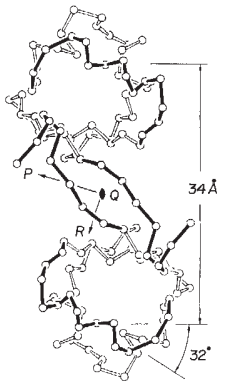

Fig. 4 Dimer of two cro molecules viewed along the Q symmetry axis. The P and R symmetry axes are also shown. Regions of the protein backbone closest to the viewer, and presumed to interact with DNA, are drawn solid. These regions include two α-helices, 34 Å apart, inclined at 32°, and also a pair of extended strands close to the Q-axis.

by Church *et al.*[27]. The four C-terminal residues of the 2-fold-related cro monomers, which are disordered in the crystals, and also, presumably, in solution, could also interact with the DNA (Figs 5, 6, 7). Such interactions could include Lys 62 and Lys 63. Presumably these C-terminal arms, which extend in solution like 'feelers', occupy well defined positions when complexed with the DNA. The finer details of the interactions between the cro repressor and its specific operator sequences are now being explored by more careful model building, and will be described elsewhere.

The proposed binding of cro to DNA explains many of the known properties of the complex. A tetramer or a dimer of cro bound to DNA extends over exactly 17 base pairs, the length of one operator (Figs 3, 5). The mode of interaction between protein and DNA is consistent with the approximate 2-fold symmetry of the operator sequence, and the symmetry of the protein. Also, the proposed binding explains, within the present level of detail, the chemical protection experiments (Figs 3, 6). Furthermore, there is a space of ~20 Å between cro molecules bound to adjacent operators, consistent with non-cooperativity of binding[28].

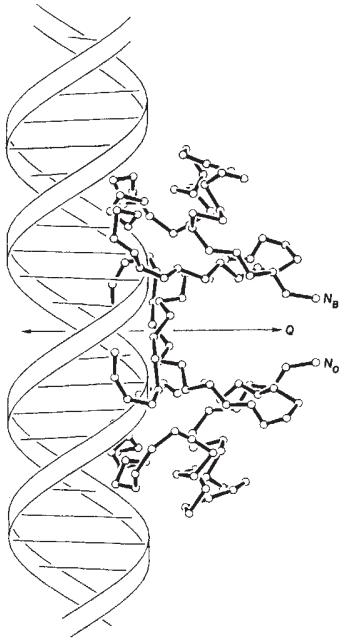

Fig. 5 Presumed interaction of cro repressor with DNA. Two monomers of cro (O and B), related by 2-fold symmetry axis Q, interact with the DNA so that axis Q coincides with the 2-fold symmetry axis of the DNA. The DNA has been rotated 90° relative to that in Fig. 3 so that its 2-fold symmetry axis is in the plane of the paper. The respective amino termini of the two cro molecules are labelled N_O and N_B. A pair of 2-fold-related α-helices occupy successive major grooves of the DNA and, closer to the symmetry axis, two extended polypeptide strands run parallel to the backbone of the DNA.

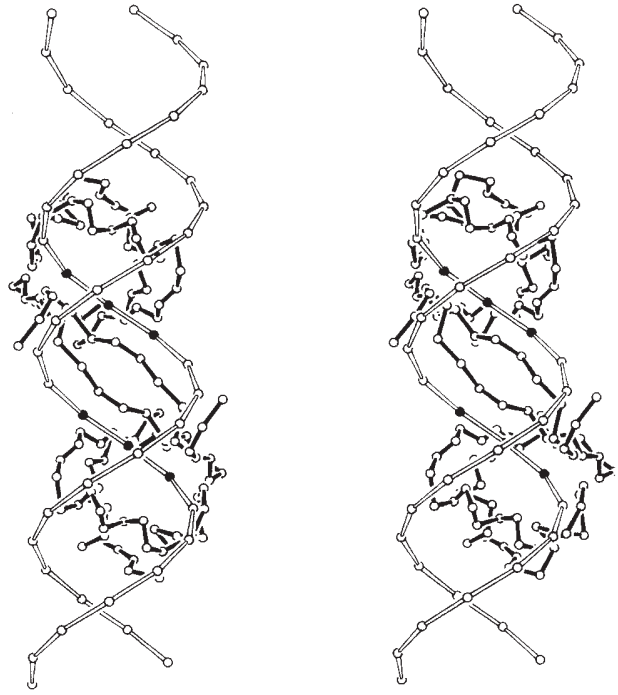

Fig. 6 Stereo view of the presumed interaction between two molecules of cro repressor and DNA, viewed along their common 2-fold symmetry axis. The open circles along the DNA backbone indicate the positions of the phosphates; those phosphates whose ethylation hinders cro binding (Fig. 3) are drawn solid.

Conclusions

This is the first structure determination of a specific DNA repressor, and the results obtained here may be of general relevance for interactions between proteins and DNA.

A principal feature of the proposed binding of cro to DNA is the use of symmetry. The 2-fold symmetry axis of the repressor coincides with the 2-fold symmetry axis of the DNA operator. This type of interaction is expected to be of general significance for proteins which recognize symmetric, sequence-specific regions of the DNA. Departures from exact symmetry could be important in 'fine tuning' of the strength of the DNA-protein complex. Our results indicate that the symmetric sequences often used for specific DNA–protein interactions are a consequence of the oligomeric structure of the regulatory proteins rather than the source of a special type of DNA structure.

Also, the α-helical conformation of proteins may presumably be used in both specific and nonspecific DNA binding. Sung and Dixon[29] were the first to propose that the histone H4 N-terminus adopts a helical conformation when interacting with chromatin nucleic acid. A related model has been proposed for *lac* repressor[30]. Also, Warrant and Kim[31] have presented direct evidence showing that protamine changes to an α-helical conformation on binding to a double-helical portion of crystalline tRNA. The cro repressor structure supports the notion that the binding of α-helices in the major groove of DNA may be a principal determinant in nonspecific protein binding to DNA, and is also of importance in specific recognition.

The structure of cro, and its complementarity to the B-form of DNA, suggest that the DNA retains the right-handed B-conformation when the repressor is bound. Of course, slight deformations of the DNA or protein could well occur on binding, and may be suggested by detailed model-building experiments, but the present results indicate that large adjustments in the DNA structure are not required to accommodate the protein. In contrast, McKay and Steitz[32] have recently proposed that the cyclic AMP receptor protein of *Escherichia coli*, which promotes the action of RNA polymerase, binds to left-handed DNA. In the case of the cro repressor, the protein is located

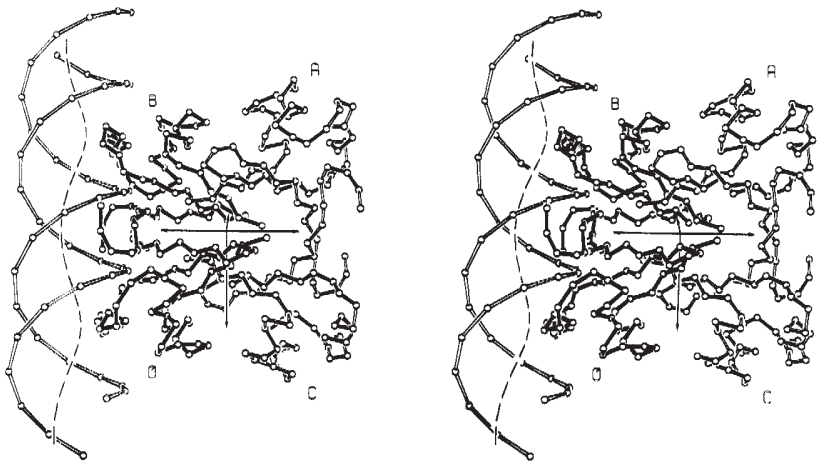

Fig. 7 Stereo view of the presumed binding of a tetramer of cro to DNA. Monomers O and B, seen interacting with the DNA, are drawn with solid bonds, whereas monomers A and C which form a second potential DNA binding region on the opposite side of the tetramer, are drawn with open bonds. The broken line follows the 'bottom' of the major groove of the DNA. The DNA and protein have been rotated 30° about the horizontal axis so that the direction of view is essentially along the major groove of the DNA.

against one side of the DNA, with most of the specific recognition occurring between side chains of the protein and the parts of the bases that are exposed in the major groove of the DNA. There is no apparent need to expose the bases further to facilitate recognition.

We thank Drs Howard Schachman and Harrison Echols for their help in instigating this project. We also thank our colleagues, in particular D. Bacon, R. G. Fisher, I. Herskowitz, M. F. Schmid, G. R. Smith, L. F. Ten Eyck and L. H. Weaver, for assistance and advice. This work was supported in part by grants from the NSF (PCM-8014311), the NIH (GM 20066; GM 28138), the MRC of Canada and the M. J. Murdock Charitable Trust. D.H.O. was supported by a Damon Runyan–Walter Winchell Cancer Fund Postdoctoral Fellowship (DRG-303-F).

Received 10 December 1980; accepted 18 February 1981.

1. Echols, H. *A. Rev. Genet.* **6**, 157–190 (1972).
2. Herskowitz, I. *A. Rev. Genet.* **7**, 289–323 (1973).
3. Ptashne, M. *et al. Science* **194**, 156–161 (1976).
4. Ptashne, M. *et al. Cell* **19**, 1–11 (1980).
5. Johnson, A., Meyer, B. J. & Ptashne, M. *Proc. natn. Acad. Sci. U.S.A.* **75**, 1783–1787 (1978).
6. Takeda, Y. *J. molec. Biol.* **127**, 177–191 (1979).
7. Folkmanis, A., Takeda, Y., Simuth, J., Gussin, G. & Echols, H. *Proc. natn. Acad. Sci. U.S.A.* **73**, 2249–2253 (1976).
8. Takeda, Y., Folkmanis, A. & Echols, H. *J. biol. Chem.* **252**, 6177–6183 (1977).
9. Hsiang, M. W., Cole, R. D., Takeda, Y. & Echols, H. *Nature* **270**, 275–277 (1977).
10. Roberts, T. M., Shimatake, H., Brady, C. & Rosenburg, M. *Nature* **270**, 274–275 (1977).
11. Green, D. W., Ingram, V. M. & Perutz, M. F. *Proc. R. Soc.* A**225**, 287–307 (1954).
12. Matthews, B. W. in *The Proteins* Vol. 3. 3rd edn (eds Neurath, H. & Hill, R. L.) 403–590 (Academic, New York, 1977).
13. Blundell, T. L. & Johnson, L. N. *Protein Crystallography* (Academic, London, 1976).
14. Anderson, W. F., Takeda, Y., Echols, H. & Matthews, B. W. *J. molec. Biol.* **130**, 507–510 (1979).
15. Anderson, W. F., Takeda, Y., Ohlendorf, D. H. & Matthews, B. W. *Proc. 7th Katzir-Katchalsky Conf. on Structural Aspects of Recognition and Assembly in Biological Macromolecules* March 1980 (in the press).
16. Schmid, M. F. *et al. Acta crystallogr.* (in the press).
17. Molnar, C. E., Barry, C. D. & Rosenberger, F. U. *Tech. Memo. No. 229* (Computer Systems Laboratory, Washington University, St. Louis, 1976).
18. Blow, D. M. & Crick, F. H. C. *Acta crystallogr.* **12**, 794–802 (1959).
19. Bricogne, G. *Acta crystallogr.* A**30**, 395–405 (1974).
20. Richards, F. M. *J. molec. Biol.* **37**, 225–230 (1968).
21. Colman, P. M., Jansonius, J. N. & Matthews, B. W. *J. molec. Biol.* **70**, 701–724 (1972).
22. Maniatis, T. *et al. Cell* **5**, 109–113 (1975).
23. Flashman, S. M. *Molec. gen. Genet.* **166**, 61–73 (1978).
24. Meyer, B. J., Maurer, R. & Ptashne, M. *J. molec. Biol.* **139**, 163–194 (1980).
25. Watson, J. D. & Crick, F. H. C. *Nature* **171**, 737 (1953).
26. Arnott, S. & Hukins, D. W. L. *Biochem. biophys, Res. Commun.* **47**, 1504–1509 (1972).
27. Church, G. M., Sussman, J. L. & Kim, S. -H. *Proc. natn. Acad. Sci. U.S.A.* **74**, 1458–1462 (1977).
28. Johnson, A., Meyer, B. J. & Ptashne, M. *Proc. natn. Acad. Sci. U.S.A.* **76**, 5061–5065 (1979).
29. Sung, M. T. & Dixon, G. H. *Proc. natn. Acad. Sci. U.S.A.* **67**, 1616–1623 (1970).
30. Adler, K. *et al. Nature* **237**, 322–327 (1972).
31. Warrant, R. W. & Kim, S. H. *Nature* **271**, 130–135 (1978).
32. McKay, D. & Steitz, T. A. *Nature* **(this issue)**.
33. Herskowitz, I. & Hagen, D. *A. Rev. Genet.* **14**, 399–445 (1980).
34. Echols, H. in *The Molecular Genetics of Development* (eds Loomis, W. & Leighton, T.) 1–16 (Academic, New York, 1980).
35. Johnson, A. thesis, Harvard Univ. (1980); and manuscript in preparation.

LETTERS

Solar quiescent prominences at 10.7 GHz

R. N. Bracewell

Electrical Engineering Department, Stanford University, Stanford, California 94305, USA

W. Graf

SRI International, Menlo Park, California 94025, USA

Filaments on the Sun, which are dark linear features in the light of the Fraunhofer Hα line, are a mysterious feature of the solar surface. They are blade-like extensions of the chromosphere projecting to a height of 40,000 km into the corona, and may extend for up to 200,000 km along the surface. The fact that they may persist for a year or so, disappear abruptly and then reappear in the same positions shows that they are superficial indicators of deeper phenomena. There have been several reports[1–4] of reduced brightness in the radio spectrum associated with the Hα filaments, leading to the widely accepted view that filaments are associated with broad dark radio features. This picture is, however, contradicted by our observations at 10.7 GHz of one solar filament during the solar eclipse of 12 October 1977.

Although the filaments are very thin, subtending about 8 geocentric arc s when seen vertically, nevertheless, "regions of reduced radio brightness situated above filaments" were detected[1] in 1959 and explained in terms of "relatively cold prominences which are optically thick to 8-mm radiation". Later attempts to discern filaments at radio wavelengths succeeded due to use of the 11 m mm-wave telescope at Kitt Peak and the 42 m telescope at Green Bank[2–4]. In all cases temperature depressions in the neighbourhood of filaments were reported. Khangil'din's[1] interpretation was absorption in the filamentary material; Drago and Felli[4] suggested that the temperature defect arose from lack of coronal emission from the volume occupied by the filament. The width of the depression was confirmed at ~2 arc min by Straka *et al.*[5] who proposed a model where the filament would exhibit a greater brightness temperature because the enhanced density within the filament would raise the height of the emission region. The general depression previously reported would then be due to the low-density 'cavity' surrounding the filament. Observations[6] with the 100-m telescope at Effelsberg again confirmed the temperature depression. The depression was explained in terms of 'radio filament' for the 'temperature depressions' or 'absorption features' even though the width was perhaps five times larger than that of the dark optical filament. This interpretation in terms of absorption disagreed with Straka *et al.*'s model[5] of the cavity concept because Kundu *et al.*[6] believed that the cavity model

0028–0836/81/180758—02$01.00